

# Dynamics and thermodynamics of Ibuprofen conformational isomerism at the crystal/solution interface.

Veselina Marinova,<sup>†</sup> Geoffrey P. F. Wood,<sup>‡</sup> Ivan Marziano,<sup>¶</sup> and Matteo  
Salvalaglio<sup>\*,†</sup>

<sup>†</sup>*Thomas Young Centre and Department of Chemical Engineering, University College  
London, London WC1E 7JE, UK.*

<sup>‡</sup>*Pfizer Worldwide Research and Development, Groton Laboratories, Groton, Connecticut  
06340, USA*

<sup>¶</sup>*Pfizer Worldwide Research and Development, Sandwich, Kent CT13 9NJ, UK*

E-mail: [m.salvalaglio@ucl.ac.uk](mailto:m.salvalaglio@ucl.ac.uk)

## Abstract

Conformational flexibility of molecules involved in crystal growth and dissolution is rarely investigated in detail, and usually considered to be negligible in the formulation of mesoscopic models of crystal growth. In this work we set out to investigate the conformational isomerism of ibuprofen as it approaches and is incorporated in the morphologically dominant  $\{100\}$  crystal face, in a range of different solvents - water, 1-butanol, toluene, cyclohexanone, cyclohexane, acetonitrile and trichloromethane. To this end we combine extensive molecular dynamics and well-tempered metadynamics simulations to estimate the equilibrium distribution of conformers, compute conformer-conformer transition rates, and extract the characteristic relaxation time of the conformer population in solution, adsorbed at the solid/liquid interface, incorporated in the crystal in contact with the mother solution, and in the crystal bulk. We find that, while the conformational equilibrium distribution is weakly dependent on the solvent, relaxation times are instead significantly affected by it. Furthermore, differences in the relaxation dynamics are enhanced on the crystal surface, where conformational transitions become slower and specific conformational transition pathways are hindered. This leads to observe that the dominant mechanisms of conformational transition can also change significantly moving from the bulk solution to the crystal interface, even for a small molecule with limited conformational flexibility such as ibuprofen. Our findings suggests that understanding conformational flexibility is key to provide an accurate description of the solid/liquid interface during crystal dissolution and growth, and therefore its relevance should be systematically assessed in the formulation of mesoscopic growth models.

# 1 Introduction

Crystallisation is a key step in the production of active pharmaceutical ingredients (APIs) as it can determine their purity, bulk structure, and size and shape distributions. Crystal habits of APIs are known to affect their mechanical properties and bulk density,<sup>1,2</sup> as well as their dissolution rates and consequently, their bioperformance.<sup>3,4</sup> The shape of crystal particles also impacts their compaction properties<sup>5</sup> and handling in powder form with flakes and needles being the most difficult to process.<sup>6</sup> A number of factors affect crystal growth from solution such as, the identity of the solvent, presence of impurities and cooling rate. The modification of the crystal habit of organic molecules by changing the solvent has been extensively studied,<sup>7-9</sup> stressing the importance of crystal habit prediction for optimal process and product design.<sup>10</sup>

The shape of a crystal grown from solution is determined by the relative growth rate of individual crystal faces exposed to the solvent. Crystal faces of great morphological importance grow slowly compared to other faces, whilst faces characterised by a small surface area are fast-growing. Being able to predict crystal shapes depends on obtaining reliable information on the growth kinetics of individual faces, either through molecular simulations or energy approximations in mathematical models.<sup>11</sup> Over the last few decades significant progress has been made in the accurate prediction of solution grown crystal shapes and a number methods have been developed, some of which have the capability of accounting for solvent effects. The state of the art in this field comprises of approaches relying on mechanistic models or molecular simulations. In particular, the most recent contribution in the area of mechanistic models is represented by the work of J. Li and M. Doherty.<sup>12</sup> In their work the authors introduce a mechanistic spiral growth (MSG) model to predict the steady state morphologies of a paracetamol crystal, grown from 30 different solvents. The method comprises of kink rate and kink density calculations, as well as solvent interaction calculations. The predicted morphologies match the experimental shapes very well for the cases of vapour and water growth, demonstrating the accuracy of the theory. In turn,

molecular dynamics (MD) simulations are invaluable for exploring the dynamic evolution of systems of interest, though at times the domain of applicability of MD can be limited by sampling.

In current crystal shape prediction methods conformational flexibility is typically neglected. In fact, a general approach to the systematic incorporation of conformational flexibility in crystal growth models is still missing.<sup>13</sup> In this work we aim to highlight how, even for relatively small molecules, conformational flexibility and crystal growth/dissolution are inherently coupled. To tackle this problem we analyse the conformational flexibility of a single ibuprofen molecule in four states along its path of incorporation into the crystal bulk. We choose to focus on a single molecule as a conformationally flexible unit rather than making an assumption on the nature of the growth unit involved in the process. The four states are depicted in Figure 1 and include: bulk solution, surface adsorbed, within the outer crystal surface layer and in the bulk of the solid. For all states we investigate how the solvent, as well as the structure of a crystal/solution interface, impacts ibuprofen conformational transition kinetics, thermodynamics and mechanisms. Our work paves the way towards a formulation of solvent-dependent kinetic models for the growth and dissolution of flexible molecules, necessary to predict crystal shape evolution in systems of practical relevance.

## 2 Methods

In the present study we investigate the conformational flexibility of ibuprofen in four different states, as described in Figure 1, using all-atom MD simulations. Since results from MD are only meaningful when all energetically relevant configurations have been explored, in certain cases MD is combined with well-tempered metadynamics (WTmetaD)<sup>14</sup> for computational efficiency. State-to-state kinetics and conformational rearrangement mechanisms are then reconstructed within the theoretical framework of Markov State Models (MSM).<sup>15</sup>

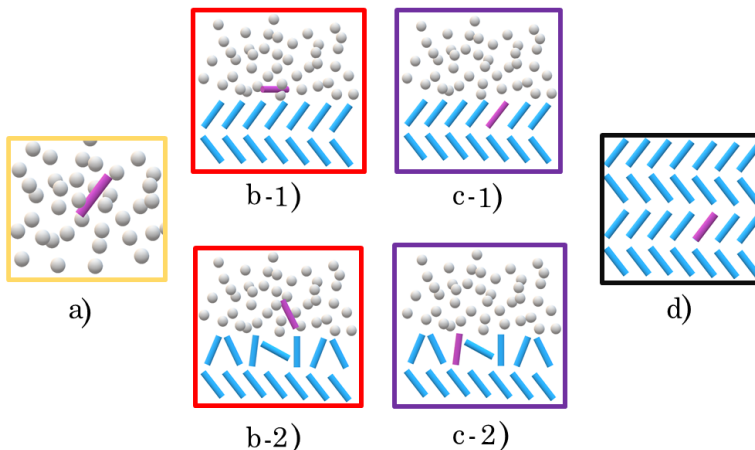


Figure 1: Scheme of states of an ibuprofen molecule along the process of incorporation in the crystal bulk - in the bulk solution (yellow frame), surface adsorbed, on an ordered or disordered surface (red frame), within the outer crystal surface layer of an ordered or disordered surface (purple frame), in the bulk of the solid (black frame).

## 2.1 Simulation setup

MD simulations were performed with Gromacs 5.1.4<sup>16</sup> using the Generalised Amber Force Field (GAFF)<sup>17</sup> and an explicit representation of the solvent. Force field parameters for solvent molecules were obtained from the Virtual Chemistry solvent database.<sup>18,19</sup> Where relevant, WTmetaD and collective variable post-processing have been carried out using Plumed 2.3<sup>20</sup>.

Seven solvents were considered in this study - water, 1-butanol, toluene, cyclohexanone, cyclohexane, acetonitrile and trichloromethane. The conformational complexity of the ibuprofen molecule was considered for each solvent in a surface state, an adsorbed state and in solution. In our study we have considered the morphologically dominant  $\{100\}$  crystal face. Due to the layered character of the  $\{100\}$  face and depending on where a slice is made, either polar or apolar functionalities may be exposed to the external environment, as shown in Figure 2. In the present study we investigate both scenarios for each solvent, as discussed in detail in the results section.

The kinetic and thermodynamic information in each case was recovered using independent simulations. In addition, kinetics recovered with the aid of metadynamics involved

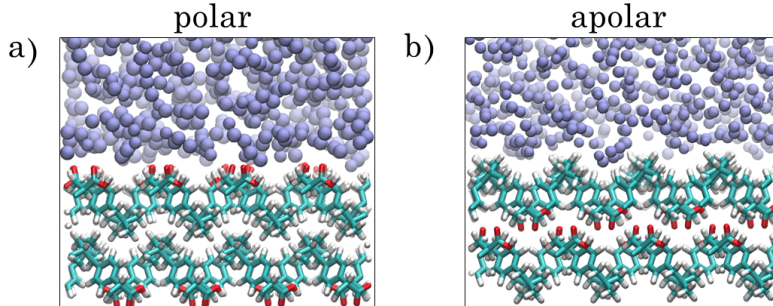


Figure 2: **a)** Ibuprofen  $\{100\}$  polar surface (left) and **b)** ibuprofen  $\{100\}$  apolar surface (right), where solvent molecules are represented as spheres for simplicity.

performing 50 simulations per starting configuration. For a detailed summary of the number and the type of simulations performed for each case, please refer to Section A of the Supplementary Material.

**Molecular Dynamics Setup** Prior to MD, each system undergoes an energy minimisation using a conjugate gradient algorithm with a tolerance on the maximum residual force of  $100 \text{ kJ mol}^{-1} \text{ nm}^{-1}$ . In all MD simulations a cut-off of 1.0 nm for non-bonded interactions is chosen, three-dimensional periodic boundary conditions (*abc*) are applied and long range intermolecular interactions are included using the particle-mesh Ewald (PME) approach.<sup>21</sup> A time step of 2 fs was used in conjunction with constraining the fast bond vibrations by applying the LINCS algorithm.<sup>22</sup> All of the simulations analysed in this work were carried out within the isothermal-isobaric (NPT) ensemble at pressure of 1 bar and temperature of 300 K, using Bussi-Donadio-Parrinello thermostat<sup>23</sup> and Berendsen barostat.<sup>24</sup> Coupling between the x, y and z components in the barostat setup is varied based on the environment in which the conformational flexibility of ibuprofen is investigated. A fully isotropic pressure control is used for bulk solution simulations. For simulations in the crystal bulk, we apply an anisotropic pressure scaling, in order to explicitly account for any potential deformation of the crystal lattice induced by local conformational transitions. Simulations of the solid/liquid interface are carried out by using a semi-isotropic pressure control, as it allows the continuous adaptation of the system volume by scaling only the z-coordinate,

avoiding rescaling distances on the x,y plane, which could destabilise the crystal slab.

**Collective Variables** The conformational ensemble of ibuprofen is mapped on a two-dimensional collective variable (CV) space, defined by two internal torsional angles that represent a *global* and *local* rearrangement of the ibuprofen molecular structure. As shown in Fig. 3, the global torsion captures the relative orientations of the *para*-substituents with respect to one another around the plane of the phenyl ring, whereas the local torsion captures the relative rotational angle of the methyl groups of the isobutanyl substituent.

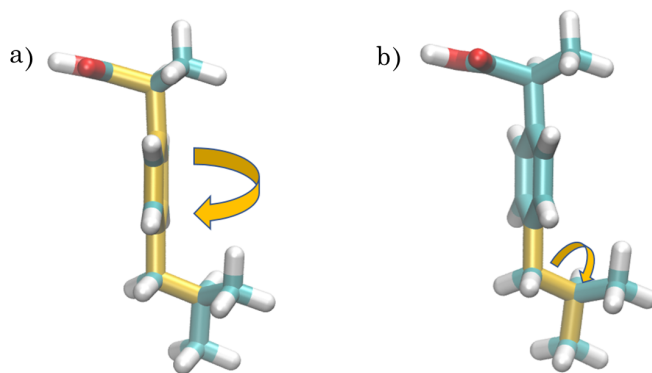


Figure 3: Internal torsional angles of ibuprofen used to map the conformational space of the molecule. a) Global torsional angle monitors the rotation of the methyl groups around the vertical axis of the molecule and b) Local torsional angle monitors the degree of interchange between the methyl groups.

For a quantitative assessment of the crystal/solution interface structural rearrangement we define an order parameter (SMAC) that captures the local order within the coordination sphere of an ibuprofen molecule. SMAC is based on the evaluation of the density of the first coordination shell and on the relative orientation of neighbours, considering the bulk crystal structure as a reference. Details for the mathematical definition of SMAC can be found in Ref.<sup>25</sup> and.<sup>26</sup> The SMAC parameters used for ibuprofen in the present study are reported in Section B in the Supplementary Material.

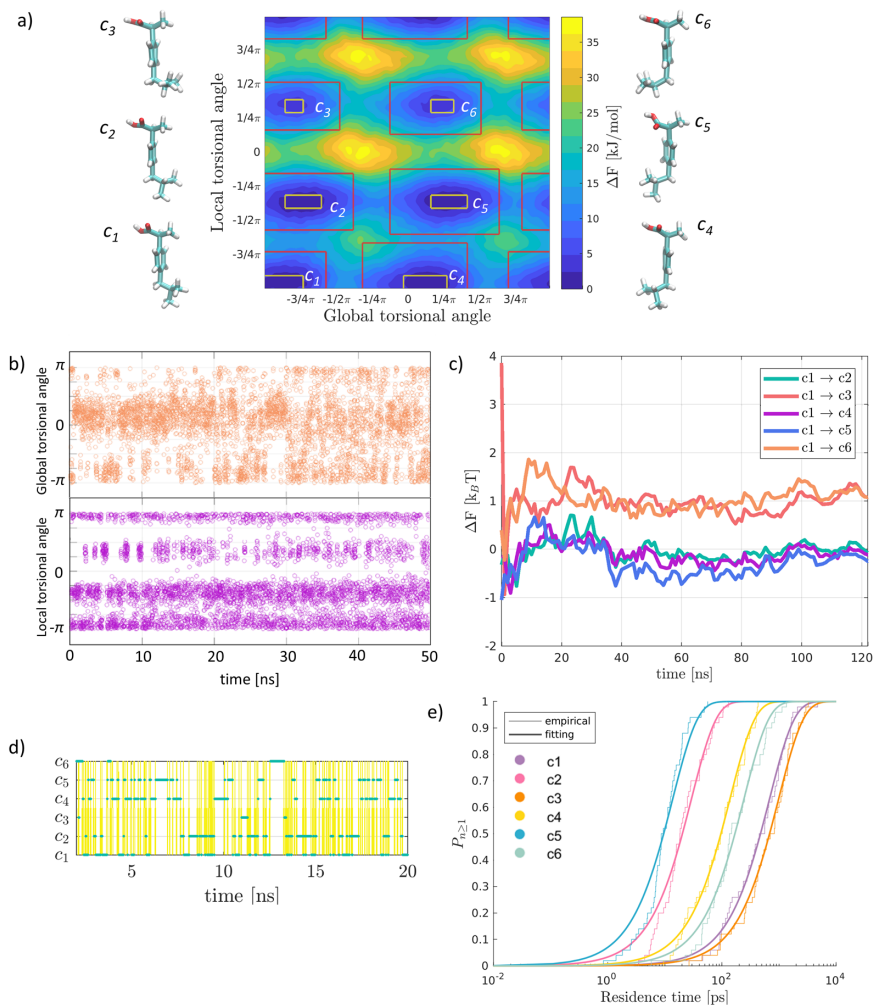


Figure 4: **a)** Free energy surface in the conformational space of the two internal torsional angles of ibuprofen showing the integration domain used for calculating equilibrium distributions from WTmetaD in red and the core set domain in yellow. Molecular structures of the conformers identified by the local minima are reported alongside the FES. **b)** Global (orange) and Local (purple) torsional angle vs. time in a WTmetaD simulation **c)** Convergence of free energy differences of conformers with respect to c1. **d)** State to state transitions in an unbiased MD simulation. **e)** Conformer lifetime distribution for an ibuprofen molecule in the apolar  $\{100\}$  surface in water, recovered with the aid of WTmetaD.

**WTmetaD Setup** WTmetaD has been used as a tool to increase the sampling efficiency of ibuprofen conformational space,<sup>14</sup> as shown for a representative simulation trajectory in Fig. 4b). This allows us to compute free energy surfaces (FES) in CV space, and to estimate the rate of rare conformational transitions.<sup>27</sup> In WTmetaD simulations an external time-dependent biasing potential is introduced as a function of the torsional angle CVs discussed earlier. The external bias potential is defined as a sum of Gaussian functions. The height and width of the Gaussian functions, the pace of bias update and the bias factor are the parameters controlling the construction of the bias potential.<sup>28</sup> In Tab. 1 we report the parameters used for simulations to construct the free energy surface of the conformational space of ibuprofen, as well as for simulations used to calculate rates of conformational transitions.

Table 1: Parameters in WTmetaD simulations, used to compute free energy surfaces (FES) and conformational transition rates.

	<b>Width</b> [ rad ]	<b>Height</b> [ $k_B T$ ]	<b>Bias Factor</b> [K]	<b>Pace</b> [steps]
FES	0.1	0.96	10	500
Rates	0.1	0.24	5	1500

**Conformational equilibrium probability distribution from WTmetaD** The FES computed in collective variables space  $F(\mathbf{S})$  provides information on the equilibrium probability density  $p(\mathbf{S})$ , defined as:

$$p(\mathbf{S}) = \frac{e^{-\beta F(\mathbf{S})}}{\int_{\Omega} e^{-\beta F(\mathbf{S})} d\mathbf{S}} \quad (1)$$

where  $\Omega$  indicates the entire configuration space, and  $\beta^{-1} = k_B T$ , where  $k_B$  is the Boltzmann constant. The FES projected in the space of the global and local torsional CVs can therefore be used to compute the equilibrium probability of different conformers. For instance, as shown in the Fig. 4a), a typical FES displays a set of local minima. Each minimum corresponds to the projection in CV space of an ensemble of configurations that can be identified as a single ibuprofen conformer. Hence, by integrating the probability density  $p(\mathbf{S})$  over the

sub-domain corresponding to a local minimum in CV space, one can obtain the equilibrium probability of the conformer corresponding to that minimum. For the generic conformer  $i$ , the equilibrium probability  $P_i$  is computed as:

$$P_i = \int_{\Omega_i} p(\mathbf{S}) d\mathbf{S}n \quad (2)$$

where  $\Omega_i$  indicates the region of CV space pertaining to conformer  $i$ . The integration domains of each conformer have been indicated in Fig.4a) in red. The free energy difference between any pair of  $i$  and  $j$  conformers is therefore computed as  $\Delta F_{i,j} = -\beta^{-1} \log \frac{P_j}{P_i}$ . The convergence of WTmetaD simulations has been systematically assessed by monitoring free energy differences between conformers as a function of simulation time, as shown in Fig.4c). Each simulation is considered converged once the fluctuations in the free energy between the minimum corresponding to conformer c1 and all other conformers are less than 5 kJ mol<sup>-1</sup>. In the cases in which the sampling of the conformational space has been restricted through the application of a static bias potential, an appropriate reweighting of the results has been carried out.

**Kinetics from WTmetaD** Performing metadynamics with the aim of obtaining conformational transition kinetics requires constructing bias to favour the escape from a local free energy minimum without perturbing the transition state ensemble. This is typically achieved by reducing the pace of bias construction,<sup>27</sup> and by comparing the shape of the transition times distribution with that of an exponential distribution implied by the *law of rare events*,<sup>29</sup> as shown in Figure 4e). In this work we carry out this process by constructing distributions of transition times from 50 events obtained from independent WTmetaD simulations. Results of the Kolmogorov-Smirnov test, employed to analyse the shape of the distribution of transition times, are reported in Tab. VI in the Supplementary Material.

## 2.2 Construction of a Markov State Model

**Equilibrium probability and system relaxation time** In this work we are interested in using a Markov State Model (MSM) to compute the global relaxation time of the conformational population, the mechanism of conversion between conformers, and their equilibrium populations. Each macrostate in the MSM represents an ensemble of configurations, corresponding to a stable ibuprofen conformer.

These conformers have been identified by analysing the local minima of the FES obtained by sampling the CV space with WTmetaD. The choice of an enhanced sampling method such as WTmetaD allows to efficiently sample all conformers even in conditions where transitions are extremely rare such as in the crystal bulk. Furthermore, the equilibrium populations obtained from WTmetaD provide a completely independent estimate of the equilibrium distribution, which we have used to cross-validate results obtained from MSMs constructed from multiple unbiased simulations (see the Supplementary Material, Section F).

An MSM is defined by a master equation of the following form:

$$\dot{\mathbf{P}}(t) = \mathbf{K}\mathbf{P}(t) \tag{3}$$

where  $\mathbf{P}(t)$  is the vector with the probabilities of each macrostate at time  $t$ , and  $\mathbf{K}$  is a transition rate matrix which has off-diagonal elements  $k_{ij} \geq 0$  and diagonal elements  $k_{ii} = -\sum_{j \neq i} k_{ji} < 0$ .<sup>15,30</sup>

Elements of the transition rate matrix can be computed either from unbiased simulations or from metadynamics, depending on the inherent timescale of the process.<sup>31,32</sup> In the case of unbiased simulations we apply a lifetime-based estimate<sup>33</sup> of the transition rate from state  $i$  to state  $j$ :  $k_{ij} = \tau_i^{-1}C_{ij}$ , in which  $\tau_i$  is the total residence time in state  $i$  and  $C_{ij}$  is the total number of transitions from state  $i$  to state  $j$ . Transitions were accounted for only when the so-called core set of state  $j$  is reached. By doing so, we avoid including non-Markovian transitions in our analysis.<sup>33</sup> Core sets for all the ibuprofen conformational

isomers are shown in Figure 4a) in yellow. A representation of state-to-state transitions within a typical trajectory is shown in Figure 4d). For the cases where it is more practical to obtain kinetic information from metadynamics for computational efficiency, individual simulations starting from each conformer were carried out. The distribution of transition times was then compared to an exponential distribution, assessing their compatibility with a Kolmogorov-Smirnov test at 95 % significance (Figure 4e).

Eq. 3 admits a unique stationary equilibrium distribution determined by:<sup>15,30,33</sup>

$$\mathbf{K}\mathbf{P}_{eq} = 0 \tag{4}$$

Solving for the eigenvalues and eigenvectors of the transition rate matrix  $\mathbf{K}$  allows us to extract equilibrium probabilities of the conformational isomers  $\mathbf{P}_{eq}$  and relaxation times. The eigenvalues of the matrix  $\mathbf{K}$  can be sorted by magnitude:  $\lambda_1 = 0 > \lambda_2 \geq \lambda_3 \geq \dots \geq \lambda_N$ . The equilibrium population is obtained from the normalization of the left eigenvector corresponding to  $\lambda_1 = 0$ . The largest non-zero eigenvalue of the  $\mathbf{K}$  matrix,  $\lambda_2$ , corresponds to the slowest mode of the system. The relaxation (or equilibration) time that we refer to in the paper is computed as  $|\lambda_2^{-1}|$ . Since macrostates in the MSMs correspond to ibuprofen conformers, the relaxation time extracted from the model can be interpreted as the characteristic time to achieve conformational equilibration.

**Transition pathway between macrostates** An MSM is a powerful tool for studying the most likely transition pathway between any two macrostates. To this end, a knowledge of the transition probability matrix  $\mathbf{T}$  between all macrostates is required. Elements of the transition probability matrix  $T_{ij}$  can be estimated from MD simulation by computing the number of transitions between each pair of states  $i$  and  $j$ ,  $C_{ij}$ :

$$T_{ij} = \frac{C_{ij}}{\sum_{k=1}^N C_{ik}} \tag{5}$$

where  $k$  represents each of the  $N$  macrostates.

With the knowledge of the transition probability matrix, a discrete transition pathway between any two states  $A$  and  $B$  is obtained by computing the committor probability  $q_n^+$ , and the state-to-state net probability flux. The former is the probability that, when in the generic state  $n$ , which belongs to the ensemble of all intermediate states  $I$ , the system will visit state  $B$  before state  $A$ . The committor probability  $q_n^+$  is computed as:<sup>15</sup>

$$-q_n^+ + \sum_{k \in I} T_{nk} q_k^+ = - \sum T_{nB} \text{ for } n \in I \quad (6)$$

where  $k$  runs over the ensemble of all intermediate macrostates of the system. By definition, the committor probability in the starting state  $A$  is 0 and in the final state  $B$  is 1.

Once the committor probability for all states along the the discrete transition pathway between  $A$  and  $B$  is obtained, the net state-to-state probability flux between any two states  $i$  and  $j$ ,  $f_{ij}^+$ , is calculated using Eq. 7:<sup>15</sup>

$$f_{ij}^+ = \pi_i T_{ij} (q_j^+ - q_i^+) \quad (7)$$

It is important to note that the committor probability and the net probability flux are two complementary pieces of information in the study of the preferred transition pathway between macrostates. The committor probability on its own allows to identify the probability of a particular intermediate macrostate  $M$  to commit to the end state  $B$ , rather than  $A$ , should the system finds itself in that particular state  $M$ . On the other hand, the net probability flux gives the absolute probability of finding the system at a particular transition only for trajectories that successfully move from macrostate  $A$  to macrostate  $B$ . Therefore, practically, and intermediate state  $M$  can have large committor probability to  $B$  and simultaneously, the net flux of the  $M \rightarrow B$  transition can be very low or none at all, due to the fact that a successful  $A$  to  $B$  move does not occur via the intermediate state  $M$ . Considered together, the

net flux and the committor probability allow us to quantitatively identify transition pathways and to infer model-based mechanistic hypotheses, reported in the Discussion section of the paper.

### 3 Results

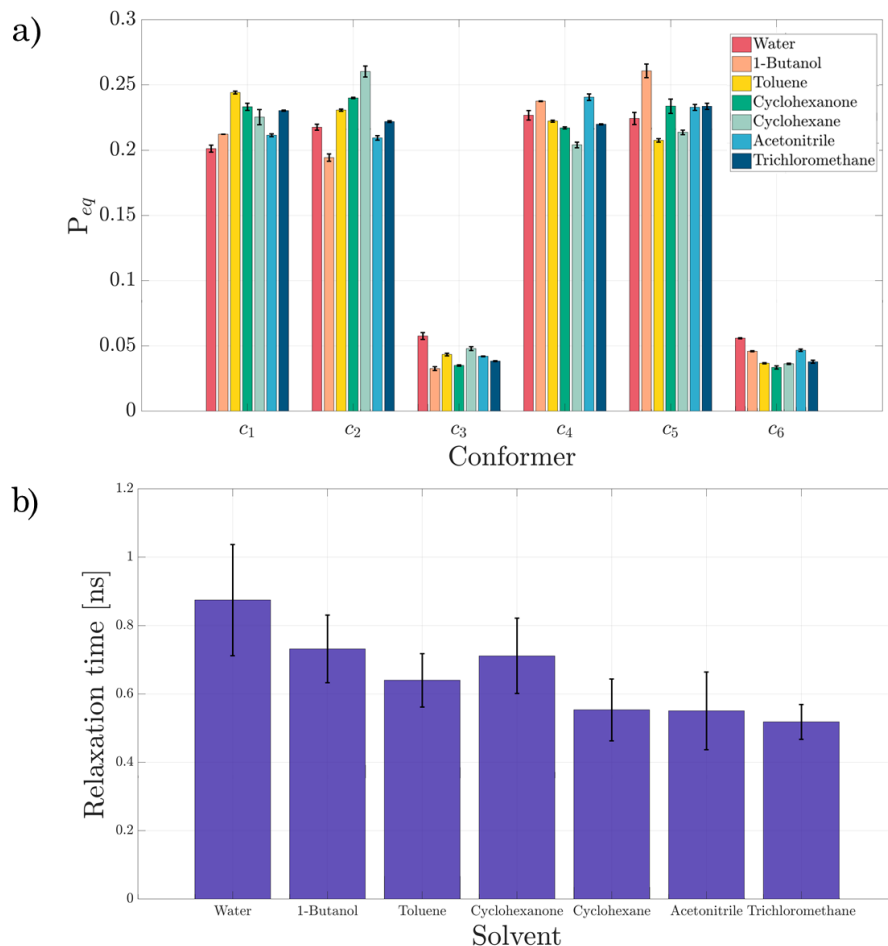


Figure 5: a) Equilibrium distribution of ibuprofen conformers in solution of different solvents recovered from WTmetaD. The solvents are shown in the order: water, 1-butanol, toluene, cyclohexanone, cyclohexane, acetonitrile, trichloromethane. Equilibrium distributions of ibuprofen conformers recovered from DFT/COSMO calculations and from MSMs are reported in the Supplementary Material (Fig. 3, Fig. 6, Fig. 7 and Fig. 8). b) Conformational equilibration times for an ibuprofen in solution obtained from MSM analysis.

In this section we report thermodynamic and kinetic results, as well as the mechanism for

the conformational transitions of ibuprofen in solution and at the morphologically dominant {100} face. In determining the crystal face with largest morphological importance we rely on BFDH model calculations, obtained using the software Mercury,<sup>34</sup> as well as experimental studies of solvent effects on the shape of ibuprofen crystals.<sup>9,35</sup> An extensive number of simulations (Supplementary Material, Section A) were performed in seven different solvents varying in size, polarity, and hydrogen bonding capabilities. The solvents considered are water, 1-butanol, toluene, cyclohexanone, cyclohexane, acetonitrile and trichloromethane.

To assess the effect of the presence of a crystal/solution interface we investigate ibuprofen conformational transitions in the four states mentioned in the introduction and sketched in Figure 1. We start by introducing the results obtained for the equilibrium distribution and relaxation kinetics of ibuprofen conformers in bulk solution, as shown in Figure 1a). In this case a single ibuprofen molecule is surrounded by solvent molecules in the absence of a crystal surface. Next, we discuss the equilibrium population of ibuprofen conformers found in the crystal bulk as shown in Figure 1d). We complete the results on the dynamics and thermodynamics of conformational transitions with reporting the states at the crystal/solution interface, such as those sketched in Fig. 1b, c). We conclude with a discussion on the mechanisms of conformational transitions obtained from the MSMs.

### **3.1 Ibuprofen in bulk solution**

#### **Equilibrium distribution of conformers in solution**

To assess the impact of solvent on the equilibrium probability of ibuprofen conformers in solution we carried out WTmetaD simulations of an isolated ibuprofen molecule, as described in the methods section. Such simulations uncovered six stable conformers present in each of the seven solvents investigated. The free energy surface for the case of an ibuprofen molecule in water is shown in Fig. 4a) with the conformers labelled c1 through to c6. A comprehensive summary of all the free energy surfaces computed, accompanied by an analysis of their convergence, is reported in Figures 9 and 10 of the Supplementary Material.

The equilibrium probability of conformers in solution, computed using Eq. 1 and 2, shows that conformers c1, c2, c4 and c5 dominate the distribution. Each of these conformational isomers contribute to approximately one fifth of the overall distribution. The remaining two conformers, c3 and c6, are significantly less probable, each accounting for 5% of the total conformer population. The lower probability of the latter two conformers can be accounted for by considering the position of the methyl groups of the iso-butanyl substituent with respect to the phenyl ring. Whilst in conformers c1, c2, c4 and c5 one of the methyl substituents is always pointing away from the molecule, in line with the central axis which contains the phenyl ring, in the case of conformers c3 and c6, the two groups are both equally close to the phenyl ring. This observation suggests that conformers c3 and c6 are much less probable due to the created steric effect. Small, but significant variations between the equilibrium probabilities of each conformer outside the calculated error are observed, indicating a weak dependence of the conformational distribution on the solvent. The equilibrium distribution of conformers identified from metadynamics was independently confirmed through a genetic search for stable structures,<sup>36</sup> coupled with free energy calculations, performed with internal gas-phase free energies calculated using Gaussian 09<sup>37</sup> in conjunction with the PBE0/6-31G(d) functional, along with solvation free energies derived from COSMO<sup>38</sup> calculations. The number of stable ibuprofen conformers and their equilibrium probability found with the DFT/COSMO procedure are in qualitative agreement with the results obtained with WTmetaD, indicating that the collective variables chosen allow to exhaustively explore the internal degrees of freedom of the molecule and that the forcefield chosen for this study does not introduce significant artefacts.

### **Relaxation Dynamics of the conformer population**

Unbiased MD simulations of an isolated ibuprofen molecule in different solvents allowed us to compute state-to-state transition probabilities and construct a Markov State Model. Stable conformational states were defined according to the position of the local free energy

minima identified in CV space. Core sets were considered to identify state-to-state transitions as reported in Fig. 4a). The equilibrium probability obtained from the MSM is in good agreement with the result obtained from WTmetaD (Supplementary Material, Fig. 6), providing a consistency check for our sampling strategy. Relaxation times were derived for each solvent from the MSM model and are reported in Fig. 5b). Relaxation times show that, while the equilibrium distribution of conformers varies only slightly between solvents, the system equilibration dynamics differs more substantially. The slowest equilibration in solution is computed in water, where the system equilibrates in just under 1 ns. The second longest time is registered for the cases of 1-butanol and cyclohexanone. In the remaining solvents relaxation times are all in the range between 0.5 - 0.7 ns . This trend of relaxation times indicates that solvent polarity and, potentially, the ability of the ibuprofen molecule to form hydrogen bonding with the solvent play a role in the interconversion dynamics of the conformational isomers of ibuprofen in solution, even if their contribution to the equilibrium distribution of conformers is more limited.

### **3.2 Equilibrium distribution and lifetime of ibuprofen conformers in the crystal bulk**

WTmetaD was also employed to sample the conformational space accessible to an ibuprofen molecule in the bulk of the crystal. The free energy surface computed for this case is reported in Fig. 6b). An analysis of the associated conformer equilibrium distribution revealed that, while conformer c1 has a 98 % probability, ibuprofen maintains a non-negligible conformational flexibility in the crystal bulk. Conformers involving a rotation along the local torsional angle can be observed and account for 2% of the equilibrium distribution. With the aid of *infrequent* metadynamics the lifetime of conformer c1 was estimated to be of the order of 100 ns. The p-value associated with the Kolmogorov-Smirnov statistic of the escape time distribution<sup>29</sup> is reported in Tab. VI in the Supplementary Material. In all of the trajectories used to compute the escape time from the local minimum corresponding to

conformer c1, the escape leads to conformer c2.

### 3.3 Equilibrium distribution and lifetime of ibuprofen conformers at the crystal-solution interface

In this section we report the results obtained for an ibuprofen molecule adsorbed on the crystal surface (state b in Fig. 1), or embedded in the surface layer in contact with the liquid solution (state c in Fig. 1). We find that the conformational population and the system equilibration times in the states at the crystal solution/interface depend on the structure of the surface, as well as on the polarity of the functional groups in contact with the solution (see Fig. 2 for polar and apolar layer descriptions). To quantify the effect of the solvent on the surface roughness and stability we use the order parameter SMAC. A detailed overview of the effect of each solvent on the behaviour of the both apolar and polar {100} crystal faces can be found in Section C of the Supplementary Material. In Tab. 2 we summarise the effect of surface-solvent interactions on the surface roughness and stability of the adsorbed state.

Table 2: Interface structure and stability of the adsorbed state for all interface/solvent combinations.

solvent	interface			
	polar		apolar	
	structure	ads. state	structure	ads. state
water	ordered	-	ordered	yes
1-butanol	disordered	yes	ordered	yes
toluene	unstable	-	ordered	-
cyclohexanone	ordered	yes	ordered	yes
cyclohexane	unstable	-	ordered	yes
acetonitrile	ordered	yes	ordered	-
trichloromethane	unstable	-	ordered	-

Free energy surfaces for an ibuprofen adsorbed on the crystal surface and embedded in the outer layer of the crystal configurations for the water/ibuprofen interface are reported in Fig. 6a), c) and d). Equilibrium probability of the c1 - c6 conformers moving from the

bulk of the liquid (water) to the bulk of the crystal are reported in Fig. 6e). Characteristic relaxation times of the conformer population for surface/adsorbed and solution states for the apolar and polar surface layers are reported in Fig. 7a) and in Fig. 7b) respectively .

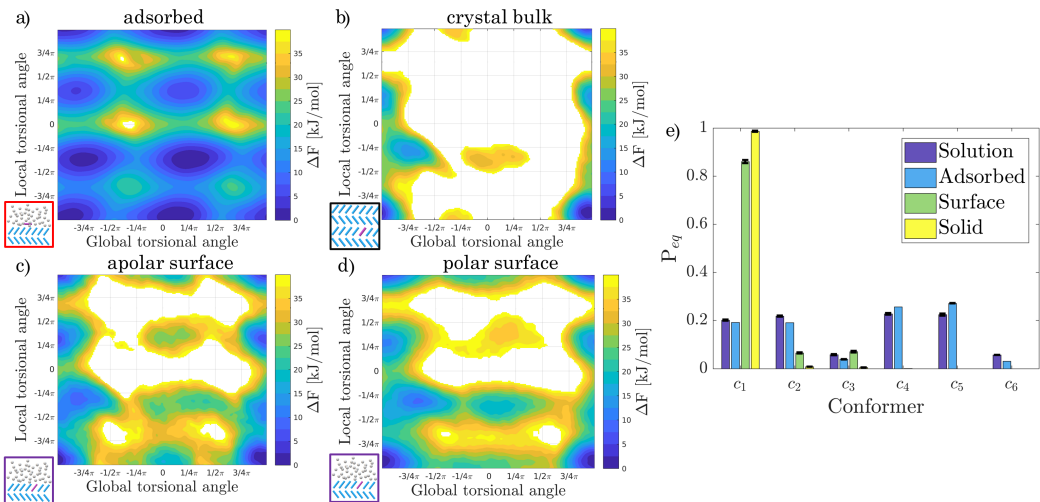


Figure 6: a-d) Free energy surfaces of an ibuprofen molecule in water, adsorbed on the solid/liquid interface (a), in the crystal bulk (b), embedded in the apolar crystal surface (c) and in the polar crystal surface (d). It can be noted that the accessible conformational space is systematically reduced as the molecule moves from solution to the crystal bulk and that the topology of the surface changes moving from the adsorbed to the surface state. e) Equilibrium probability of the six ibuprofen conformers  $c_1$  -  $c_6$ , found in the stages involving incorporation of a molecule into the crystal, considering water as a solvent and an apolar  $\{100\}$  crystal surface.

### Ibuprofen adsorbed on the crystal surface

The equilibrium distribution of ibuprofen conformers adsorbed on the  $\{100\}$  crystal surface resembles closely the distribution obtained in solution. Slightly higher probability of  $c_2$ ,  $c_4$  and  $c_5$  is observed in certain solvents (see section F of the Supplementary Material), revealing signs of conformationally-selective adsorption. MSMs were built using unbiased MD simulations for the stable adsorbed states. The model was, again, verified by comparing the equilibrium distribution from the MSM to the one recovered from WTmetaD (see Fig. 7 in Supplementary Material). The interplay between solvent and interface, however, has in this case a much more remarkable effect on the system dynamics. Relaxation times in the

adsorbed state on both surfaces show a different trend with respect to those computed in solution. For instance, in the adsorbed state equilibration is the slowest for a molecule on the polar surface in the presence of acetonitrile, 1.5 ns, followed by the case of 1-butanol of around 1.3 ns. Contrary to what is observed in the solution bulk, conformational relaxation in the adsorbed state is the fastest for the crystal/water apolar interface and is in fact counter-intuitively *faster* than the one in solution. This effect is likely to be caused by the stronger surface/molecule interaction compared to the surface/solvent interaction due to the apolar character of the surface. In addition to that, water is a small molecule and so conformational rearrangement of the adsorbed ibuprofen molecule will not be impeded by large solvent molecules. Overall, this effect creates a non-monotonic trend in the relaxation times for the case of water when moving from solution to the surface. In addition to the different arrangement of the solvents in terms of relaxation times, the conformational equilibration times occupy a broader time range and the differences between solvents are much more significant compared to the solution case as observed in Fig. 7. These kinetic observations show that the character of the surface impacts dynamics more significantly than thermodynamics, i.e. differences in the equilibrium probability of conformers in the two surfaces in fact do not exceed 10%. A complete summary of conformational relaxation times for the adsorbed state can be found in Tab. 3. These results clearly indicate that the kinetics of conformational rearrangement of adsorbed molecules are dictated by specific solvent-surface interactions, and their relaxation timescale differs from that computed in solution.

### **Ibuprofen embedded in the crystal surface**

The equilibrium distribution within the surface layer of the  $\{100\}$  crystal is dominated by the c1 conformer with an equilibrium probability higher than 80% for both the apolar and polar faces. The probability distribution suggests that rotations along the *local* torsional angle are associated to a lower energy penalty regardless of whether the CH<sub>3</sub> groups are in direct contact with the solvent. Particularly low probability for c1 is found for the case of

Table 3: Average relaxation times [ns] for the adsorbed states on polar and apolar {100} ibuprofen surface. Only cases in which the adsorbed state is stable have been reported.

solvent	Relaxation times [ns]	
	polar	apolar
water	-	0.5
1-butanol	1.3	1.3
toluene	-	-
cyclohexanone	1.0	1.0
cyclohexane	-	0.7
acetonitrile	1.5	-
trichloromethane	-	-

1-butanol in the polar surface. This is due to surface roughening, which allows for a higher conformational flexibility. (Fig. 5 in Section F of the Supplementary Material) In the case of the polar surface in acetonitrile we find that perturbing the conformational space of a surface molecule by adding biasing potential within the framework of WTmetaD causes its detachment, indicating that detachment from the surface is coupled with its conformational transition. Overall, highlighting equilibrium distribution variations between states involved in dissolution shows that embedding an ibuprofen molecule in the surface layer provides a significant conformational selectivity. In fact,  $c1 \rightarrow c4$  and  $c1 \rightarrow c5$  become so rare, that the probability of  $c4$  and  $c5$  reduces to less than 1 %. We build MSMs for all surface/solvent couples, based on the kinetics of state-to-state transitions, obtained from WTmetaD simulations. The equilibrium distribution obtained is once again in good agreement with the one from WTmetaD (Fig. 8 in the Supplementary Material), confirming the internal consistency of the results obtained.

Relaxation times computed from MSMs show that conformational equilibration times in the apolar surface increase substantially for all solvents compared to the solution case. Relaxation times range between 1 and 2 ns (2-5 times slower than in solution, see Fig. 7a), with the largest slowdown registered for the case of 1-butanol. We note that the apolar surface is ordered in all solvents considered. The overall trend in relaxation times appears therefore to be correlated to the fact that the ibuprofen molecules adopt a crystal-like configuration

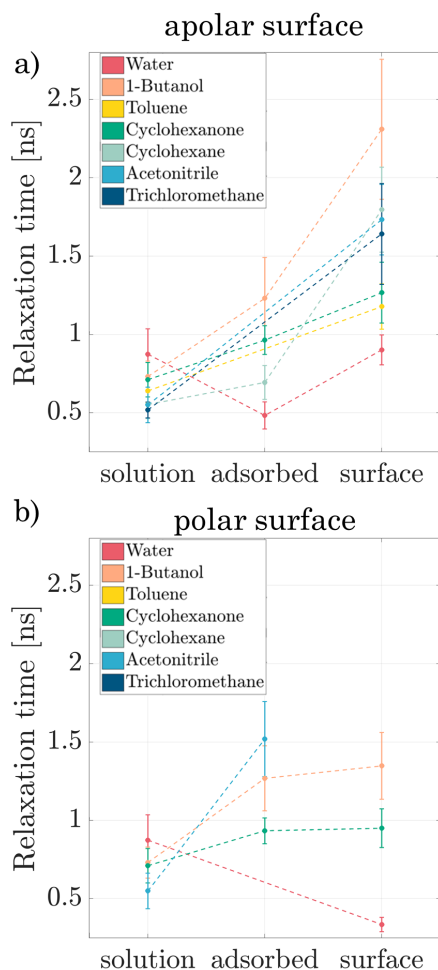


Figure 7: System relaxation times, obtained through an MSM analysis in the case of a) apolar  $\{100\}$  surface and b) polar  $\{100\}$  surface. Error bars represent the standard deviation of the relaxation time distribution obtained from bootstrapping.<sup>39</sup>

when in the surface, hindering their conformational transitions. An exception to this trend is water, which due to its hydrogen bonding, induces the slowest relaxation in bulk solution despite offering the the lowest sterical hindrance among the solvents considered.

Conformational equilibration of ibuprofen in the polar  $\{100\}$  surface slows down compared to solution, however, moving from the adsorbed to the surface state does not significantly affect the relaxation dynamics which plateaus around 1 ns (see Fig. 7b). Also in this case water represents an exception, exhibiting a relaxation time in the surface configuration which is shorter than both bulk solution and apolar surface (0.3 vs 1 ns). We note that the carboxylic moiety of ibuprofen in the polar surface is exposed to the water molecules,

which can form hydrogen bonds with it. Its accessibility however is markedly reduced when compared to bulk solution, hence the conformational equilibration becomes comparatively faster.

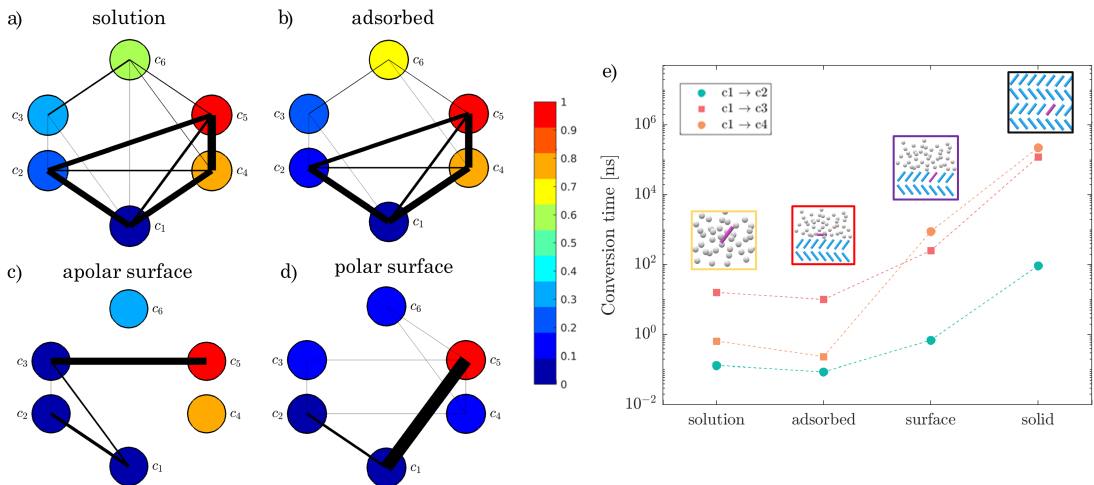


Figure 8: a) Mechanism of conversion of conformer  $c_1$  to conformer  $c_5$ , in solution (a), an adsorbed configuration on the apolar  $\{100\}$  crystal surface (b), embedded in the apolar  $\{100\}$  crystal surface (c) and in the polar  $\{100\}$  crystal surface (d). In all four cases the solvent is water. The colour of the states represents the probability of converting to conformer  $c_5$  before conformer  $c_1$ . The net probability flux from  $c_1$  to  $c_5$  is represented through line thickness. For a more detailed explanation of the committor probability and the net flux please refer to paragraph B in the Methods section. e) Conversion rates between  $c_1$  and neighbouring conformers in CV space going through the four states considered in this study. Data points marked with circles have been obtained through unbiased MD or recovered from well-tempered metadynamics, while the data points in squares have been computed using known transition rates and free energy barriers between relevant states.

### 3.4 Discussion

**Conformational equilibrium distribution** In this study the conformational flexibility of ibuprofen is investigated with the aid of MD simulations in combination with WTmetaD and the theoretical framework of the Markov State Model. In all cases we find good agreement between the equilibrium distribution obtained from WTmetaD and the MSM constructed from individual transition rates. Based on these findings we can conclude that the free energy landscape of ibuprofen conformers is strongly dependent on the environment (so-

lution, adsorbed, interface, crystal bulk) and weakly dependent on the solvent. The latter is further confirmed by the equilibrium distribution obtained with DFT/COSMO calculations, which also predict minimal variability in the equilibrium distribution of conformers in different solvents. Conformational selectivity is observed in the adsorbed state and the surface state of the ibuprofen molecule, and is particularly obvious in the crystal bulk. Despite the fact that the polar and apolar  $\{100\}$  surfaces expose different functional groups of the molecule to the solution, we find that the conformational distribution of ibuprofen in both is very similar, indicating that rotation along the local torsional angle is more energetically favourable than along the global one in both cases.

**Relaxation dynamics of the conformer population** We use MSMs to obtain the characteristic equilibration time for the population of conformers c1 - c6 in all of the states investigated. In most cases the presence of a surface only marginally slows down the global conformational rearrangement. Nonetheless, it can be concluded that the system relaxation times are both environment and solvent dependent. More importantly, there is a significant difference in the computed trends between the polar and apolar  $\{100\}$  surfaces. Whilst in the apolar  $\{100\}$  surface case the system equilibration generally increases when moving from solution to the surface, in the case of the polar surface the relaxation times remain comparable to the corresponding adsorbed states. Overall, we note that relaxation dynamics are affected by solvent properties (size, flexibility, polarity, ability to form hydrogen bonds), as well as surface characteristics (roughness, functional groups exposed to the solution) and gaining a molecular-level insight is therefore important.

**Equilibration mechanism** While the global relaxation time of the conformational population slows down only marginally, there is a clear modification in the mechanism of conformational rearrangement of ibuprofen molecules when moving from considering the bulk solution to the crystal surface. To quantify this change in terms of kinetics we investigate the escape rates from the bulk crystal conformer c1 to each of its neighbours in CV space, c1

$\rightarrow c2$ ,  $c1 \rightarrow c3$  and  $c1 \rightarrow c4$ , in all stages of incorporation with respect to the apolar  $\{100\}$  crystal slab. Transition rates that have been obtained with the aid of metadynamics and/or the analysis of unbiased MD trajectories are reported with circles in Fig. 8e). The rest of the transition rates have been calculated using the ratio of free energy barriers between states from WTMetaD calculations (indicated with squares). We find that the conversion  $c1 \rightarrow c4$  goes from being comparable to the  $c1 \rightarrow c2$  conversion in solution to being the slowest transition in the crystal surface and in bulk. This indicates that the rearrangement mechanism of conformers depends heavily on the position with respect to the crystal interface.

In order to further investigate modifications in the conformational transition mechanism, we use the MSMs to analyse a transition pathway from conformer  $c1$  to conformer  $c5$ . We find that in solution and in the adsorbed state the most likely mechanism of conversion unfolds via conformers  $c2$  and  $c4$ , as indicated by the net flux in Fig. 8a) and b). Looking at the mechanism of conversion in the surface however, we find that it is dependant on the surface-solvent interactions. For the case of an ibuprofen in the apolar surface  $c1$  to  $c5$  transition occurs exclusively via conformer  $c3$ , see Fig. 8c), whilst for the case of a polar surface the most likely mechanism is a direct transition Fig. 8d).

## 4 Conclusions

By combining extensive unbiased MD, WTMetaD and MSMs, in this study we propose a systematic approach for the identification of kinetics, thermodynamics and transition mechanisms of relevant conformational transitions of organic molecules at the crystal/solution interface.

Here we investigate conformational isomerism of ibuprofen at the solid/liquid interface. We find that the equilibrium distribution of conformers is strongly dependent on the environment of the molecule with respect to the crystal surface. When in contact with the  $\{100\}$  surface, the conformational rearrangement time generally increases moving from the solution

to the surface states, and differs between solvents. On the other hand, the conformational rearrangement in the polar  $\{100\}$  surface exhibits different kinetic behaviour and relaxation times in the surface are more similar to those in solution. We find that the specific solvent/surface interactions govern the conformational behaviour of the molecule. Moreover, in both the polar and apolar surfaces we find a change in the mechanism of conformational rearrangement with respect to bulk solution. With these results we show that, even in a moderately flexible molecule such as ibuprofen, thermodynamics, kinetics and mechanisms of conformational equilibria are significantly affected by the presence of a crystal interface and by its interplay with the solvent. This finding highlights the need to develop systematic approaches for including conformational transitions in mesoscopic models of crystal growth.

## **Conflict of interest**

There are no conflicts to declare.

## **Acknowledgements**

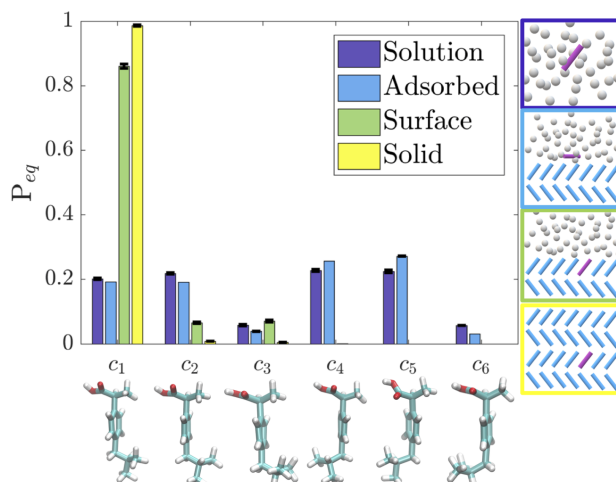
The authors acknowledge Legion High Performance Computing Facility for access to Legion@UCL and associated support services, in the completion of this work.

## **Supplementary Material**

See supplementary material for a list of simulations, the set up of the collective variables used to characterise the surface structures, a detailed description of the surface-solution interactions observed, free energy surfaces for all the states in all solvents considered, convergence of free energy differences, and conformer populations in all states computed with WTmetaD

and MSM, and conformers probability in solution computed with the DFT/COSMO procedure.

## Table of Content Graphics



## References

- (1) Hadi A. Garekani, James L. Ford, Michael H. Rubinstein, A. R. R.-S. Formation and compression characteristics of prismatic polyhedral and thin plate-like crystals of paracetamol. *Int J Pharm* **1999**, *187*, 77–89.
- (2) Garekani, H. A.; Sadeghi, F.; Badiie, A.; Mostafa, S. A.; Rajabi-Siahboomi, A. R.; Rajabi-Siahboomi, A. R. Crystal Habit Modifications of Ibuprofen and Their Physico-mechanical Characteristics. *Drug Dev Ind Pharm* **2001**, *27*, 803–809.
- (3) Hooton, J. C.; Jones, M. D.; Harris, H.; Shur, J.; Price, R. The Influence of Crystal Habit on the Prediction of Dry Powder Inhalation Formulation Performance Using the Cohesive Adhesive Force Balance Approach. *Drug Dev Ind Pharm* **2008**, *34*, 974–983.

- (4) N. Blagden, M. de Matas, P.T. Gavan, P. Y. Crystal engineering of active pharmaceutical ingredients to improve solubility and dissolution rates. *Adv Drug Deliv Rev* **2007**, *59*, 617–630.
- (5) P.V. Marshall, P. The compaction properties of nitrofurantoin samples crystallised from different solvents. *Int J Pharm* **1991**, *67*, 59–65.
- (6) Kim, S.; Wei, C.; Kiang, S. Crystallization process development of an active pharmaceutical ingredient and particle engineering via the use of ultrasonics and temperature cycling. *Org Process Res Dev* **2003**, *7*, 997–1001.
- (7) Sudha, C.; Srinivasan, K. Understanding the effect of solvent polarity on the habit modification of monoclinic paracetamol in terms of molecular recognition at the solvent crystal/interface. *Cryst Res and Technol* **2014**, *49*, 865–872.
- (8) Davey, R.J., Mullin, J.W., Whiting, M. Habit modification of succinic acid crystals grown from different solvents. *J Cryst Growth* **1982**, *58*, 304–312.
- (9) Bunyan, J.; Shankland, N.; Sheen, D. Solvent effects on the morphology of ibuprofen. *AIChE Symp. Ser.* **1991**, *284*, 44 – 57.
- (10) Variankaval, N.; Cote, A. S.; Doherty, M. F. From form to function: Crystallization of active pharmaceutical ingredients. *AIChE J* **2008**, *54*, 1682–1688.
- (11) Lovette, M. A.; Browning, A. R.; Griffin, D. W.; Sizemore, J. P.; Snyder, R. C.; Doherty, M. F. Crystal Shape Engineering. *Ind Eng Chem Res* **2008**, *47*, 9812–9833.
- (12) Li, J.; Doherty, M. F. Steady State Morphologies of Paracetamol Crystal from Different Solvents. *Cryst Growth & Des* **2017**, *17*, 659–670.
- (13) Elts, E.; Greiner, M.; Briesen, H. In Silico Prediction of Growth and Dissolution Rates for Organic Molecular Crystals: A Multiscale Approach. *Cryst.* **2017**, *7*, 288.

- (14) Barducci, A.; Bussi, G.; Parrinello, M. Well-Tempered Metadynamics: A Smoothly Converging and Tunable Free-Energy Method. *Phys Rev Lett* **2008**, *100*, 020603.
- (15) Bowman, G. R. *An Overview and Practical Guide to Building Markov State Models*; 2014; pp 7–22.
- (16) Van Der Spoel, D.; Lindahl, E.; Hess, B.; Groenhof, G.; Mark, A. E.; Berendsen, H. J. C. GROMACS: Fast, flexible, and free. *J Comp Chem* **2005**, *26*, 1701–1718.
- (17) Wang, J.; Wolf, R. M.; Caldwell, J. W.; Kollman, P. A.; Case, D. A. Development and testing of a general amber force field. *J Comp Chem* **2004**, *25*, 1157–1174.
- (18) Caleman, C.; van Maaren, P. J.; Hong, M.; Hub, J. S.; Costa, L. T.; van der Spoel, D. Force Field Benchmark of Organic Liquids: Density, Enthalpy of Vaporization, Heat Capacities, Surface Tension, Isothermal Compressibility, Volumetric Expansion Coefficient, and Dielectric Constant. *J Chem Theory Comput* **2012**, *8*, 61–74.
- (19) van der Spoel, D.; van Maaren, P. J.; Caleman, C. GROMACS molecule & liquid database. *Bioinformatics* **2012**, *28*, 752–753.
- (20) Tribello, G. A.; Bonomi, M.; Branduardi, D.; Camilloni, C.; Bussi, G. PLUMED 2: New feathers for an old bird. *Comp Phys Comm* **2014**, *185*, 604–613.
- (21) Darden, T.; York, D.; Pedersen, L. Particle mesh Ewald: An  $N \log(N)$  method for Ewald sums in large systems. *J Chem Phys* **1993**, *98*, 10089–10092.
- (22) Hess, B.; Bekker, H.; Berendsen, H. J. C.; Fraaije, J. G. E. M. LINCS: A Linear Constraint Solver for Molecular Simulations. *J Comput Chem* **1997**, *18*, 1463–1472.
- (23) Bussi, G.; Donadio, D.; Parrinello, M. Canonical sampling through velocity rescaling. *J Chem Phys* **2007**, *126*, 014101.
- (24) Molecular dynamics with coupling to an external bath. *J Chem Phys* **1984**, *81*, 3684–3690.

- (25) Giberti, F.; Salvalaglio, M.; Parrinello, M. Metadynamics studies of crystal nucleation. *IUCrJ* **2015**, *2*, 256–266.
- (26) Tribello, G. A.; Giberti, F.; Sosso, G. C.; Salvalaglio, M.; Parrinello, M. Analyzing and driving cluster formation in atomistic simulations. *Journal of chemical theory and computation* **2017**, *13*, 1317–1327.
- (27) Tiwary, P.; Parrinello, M. From Metadynamics to Dynamics. *Phys Rev Lett* **2013**, *111*, 230602.
- (28) Barducci, A.; Bonomi, M.; Parrinello, M. Metadynamics. *Wiley Interdisciplinary Reviews: Computational Molecular Science* **2011**, *1*, 826–843.
- (29) Salvalaglio, M.; Tiwary, P.; Parrinello, M. Assessing the Reliability of the Dynamics Reconstructed from Metadynamics. *J Chem Theory Comput* **2014**, *10*, 1420–1425.
- (30) Noé, F.; Chodera, J.; Bowman, G.; Pande, V.; Noé, F. An Introduction to Markov State Models and Their Application to Long Timescale Molecular Simulation, vol. 797 of *Advances in Experimental Medicine and Biology*. 2014.
- (31) Tiwary, P.; Limongelli, V.; Salvalaglio, M.; Parrinello, M. Kinetics of protein–ligand unbinding: Predicting pathways, rates, and rate-limiting steps. *Proc Nat Acad Sci* **2015**, *112*, E386–E391.
- (32) Palazzesi, F.; Salvalaglio, M.; Barducci, A.; Parrinello, M. Communication: Role of explicit water models in the helix folding/unfolding processes. *J Chem Phys* **2016**, *145*, 121101.
- (33) Buchete, N.-V.; Hummer, G. Coarse Master Equations for Peptide Folding Dynamics. *J Phys Chem B* **2008**, *112*, 6057–6069.
- (34) Macrae, C. F.; Bruno, I. J.; Chisholm, J. A.; Edgington, P. R.; McCabe, P.; Pidcock, E.; Rodriguez-Monge, L.; Taylor, R.; Van De Streek, J.; Wood, P. A. Mercury CSD 2.0

- new features for the visualization and investigation of crystal structures. *J Appl Cryst* **2008**, *41*, 466–470.
- (35) Influence of Solvent on the Morphology and Subsequent Comminution of Ibuprofen Crystals by Air Jet Milling. *J Pharm Sci* **2012**, *101*, 1108–1119.
- (36) Lauer, T. M.; Wood, G. P. F.; Farkas, D.; Sathish, H. A.; Samra, H. S.; Trout, B. L. Molecular Investigation of the Mechanism of Non-Enzymatic Hydrolysis of Proteins and the Predictive Algorithm for Susceptibility. *Biochemistry* **2016**, *55*, 3315–3328.
- (37) Frisch, M.; Trucks, G.; Schlegel, H.; Scuseria, G.; Robb, M.; Cheeseman, J.; Montgomery Jr, J.; Vreven, T.; Kudin, K.; Burant, J.; et al., Gaussian 03, revision C. 02; Gaussian, Inc. *Wallingford, CT* **2004**, *26*.
- (38) Klamt, A. The COSMO and COSMO-RS solvation models. *Wiley Interdisciplinary Reviews: Computational Molecular Science* **2018**, *8*, e1338.
- (39) Bowman, G. R.; Beauchamp, K. A.; Boxer, G.; Pande, V. S. Progress and challenges in the automated construction of Markov state models for full protein systems. *J Chem Phys* **2009**, *131*, 124101.